



UNIVERSITY OF PLOVDIV
“PAISII HILENDARSKI”

FACULTY OF PHYSICS AND TECHNOLOGY
DEPARTMENT OF "MECHANICAL ENGINEERING AND
TRANSPORT"

Mag. Eng. Miroslav Dimitrov Simov

**INCREASING THE LIFETIME OF PLASTIC MOLDING
TOOLS**

ABSTRACT

of a dissertation for the acquisition of an educational and scientific degree
"DOCTOR"

Field of higher education:

5. Technical sciences

Professional field:

5.1. Mechanical Engineering

Doctoral Program:

"Methods for Controlling and Testing Materials, Products and Equipment"

Scientific supervisor:

Assoc. Prof. Dr. Eng. Velko Slavchev Rupetsov

Plovdiv, 2025

The dissertation has a volume of 139 pages, including 93 figures, 24 tables, 1 appendix, formatted as an introduction, 6 chapters, scientific and applied contributions, a list of terms and abbreviations used, a list of the author's publications. The list of cited literature includes 137 titles.

The designations of the formulas, figures and tables in the abstract coincide with those in a dissertation paper presented at a meeting of a scientific jury.

The dissertation work was discussed and directed for defense at a meeting of the extended department council of the department of "MECHANICAL ENGINEERING AND TRANSPORT" at the "PAISII HILENDARSKI" UNIVERSITY OF PLOVDIV on October 8, 2025, Protocol No. 77.

The defense of the dissertation will take place on December 18, 2025 from 2:00 pm, "Compass" Hall of the University of Plovdiv, Rectorate, 24 Tsar Asen Street, Plovdiv.

The materials for the doctoral defense are available to those interested in the Library of "PAISII HILENDARSKI" UNIVERSITY OF PLOVDIV.

Scientific jury: Prof. Dsc. Eng. Georgi Atanasov Mishev
Prof. Dsc. Eng. Nikolay Dimitrov Menkov
Prof. Dsc. Eng. Nikolay Tontchev Tontchev
Assoc. Prof. Dr. Eng. Ventsislav Borisov Nenov
Assoc. Prof. Dr. Eng. Emil Georgiev Velev

Author: Mag. Eng. Miroslav Dimitrov Simov
Title: **INCREASING THE LIFETIME OF
PLASTIC MOLDING TOOLS**

Circulation: 30 pcs.

GENERAL CHARACTERISTICS OF THE DISSERTATION

Relevance of the problem

The use of plastic products worldwide is constantly increasing. Polymer parts are successfully replacing a large part of the metal products used in the past. The physical and mechanical properties of the polymer materials used are constantly being improved by adding special fillers. The need for ever-larger quantities of plastic products also imposes additional requirements on the wear resistance of the injection molds for them.

The working surfaces of the tools for the production of polymer parts by the injection molding method are subjected to complex loading. On the one hand, the mold is subjected to cyclic temperature fluctuations during its filling with melt, and subsequently its cooling. At the same time, the working surfaces are simultaneously loaded with friction, pressure and bending as a result of filling the mold with polymer. The glass and mineral fillers in the polymer have a strong abrasive effect on the forming surfaces. Additives for non-flammability and UV protection, combined with residual moisture in the granulate, high melt temperature and other factors have a chemical effect on the working surfaces. When the tool is opened and the part is removed, the working surfaces of the injection mold are again subjected to friction. The adhesion of the polymer to the working surfaces of the tool, as well as its shrinkage after cooling, additionally lead to high efforts required to separate the finished part from the injection mold.

In order to increase the life cycle of tools for the production of polymer parts, it is necessary to take measures to increase the wear resistance of the surface layer of the working surfaces and at the same time reduce the adhesion of the polymer to the mold walls.

Purpose and objectives of the dissertation

Based on the analysis of the current state of the problem and the conclusions drawn from it, the following was formulated:

PURPOSE OF THE DISSERTATION:

Application of methods and means to increase the service life of plastic molding tools.

This goal is achieved by solving the following tasks:

1. Study of the modern state of the problem when using plastic injection molding tools.
2. Analysis of injection mold defects.
3. Materials, methodologies and tools for experimental research.
4. Simulation of the injection molding process. Factors affecting wear and opportunities for optimization of tool design.
5. Experimental studies of wear resistance, topography of hard coating and laser welded layers on Stavax ESR steel.
6. Practical methods for restoring the performance of defective injection molds.

Research methods and tools used:

Modern research equipment was used - an Atomic-force microscope - Park Systems XE 100, Stand for research and testing of coatings SIIP-1, calo-tester, nanohardness tester Compact Platform CPX (MHT/NTN) from CSM Instruments with the ability to perform a scratch test with the Micro Scratch Tester (MST) module.

Implementation and practical applicability

The wear resistance of a Ti/TiN/TiCN multilayer coating was investigated. The topography, hardness and roughness of laser-welded layers on Stavax ESR steel were investigated. The injection molding process was simulated and the factors affecting wear were analyzed.

Publications on the topic

The main results were published in: 2 issues of Journal of the Balkan Tribological Association and 1 issue of the collection of papers Alternative Energy Sources, Materials & Technologies (AESMT'22). Two of the publications are co-authored with the scientific supervisor and one is independent.

Scope and structure of the dissertation work

The dissertation is 139 pages long, including 93 figures, 24 tables, 1 appendix, formatted as an introduction, 6 chapters, scientific and applied contributions, a list of terms and abbreviations used, a list of the author's publications. The list of cited literature includes 137 titles.

CONTENT OF THE DISSERTATION

Chapter 1. Literature review

The literature review shows that the specifics of the injection molding process and the increasing use of modified polymers with various fillers and additives lead to serious challenges to the operational life of the tools.

The main factors limiting the life of injection molds are related to the various wear mechanisms – adhesive, abrasive, corrosion and fatigue of the material. These processes are enhanced by the presence of abrasive particles (glass fibers, minerals), aggressive chemical compounds, high temperatures and cyclic loads. A special influence is also exerted by flame retardant additives, which improve the fire resistance of plastics, but at the same time can lead to the release of corrosive substances, damaging the working surfaces of the tools.

In modern practice, new materials and technologies are being developed and implemented to overcome these problems. Powder metallurgy and high-alloy tool steels, as well as the application of protective surface coatings (PVD, PACVD) significantly increase wear and corrosion resistance [86].

In conclusion, it can be summarized that increasing the service life of plastic molding tools requires a comprehensive approach - the right choice of materials, the application of modern protective coatings, the optimization of technological parameters and cooling, as well as the implementation of modern methods of maintenance and repair. These measures are essential for extending the service life of the tools and increasing the efficiency of the production process.

Chapter 2. Analysis of injection mold defects

2.1. Typical defects of injection molds

Injection molds operate under very severe conditions: high loads; high temperatures; high wear. The most common types of wear on injection molds are mechanical, corrosive, abrasive, thermal, and material fatigue. They often interact with each other, thus being cumulative [9].

The analysis of the resulting defects of the injection molds was made on the basis of a study of the operation of these tools at Arexim Engineering EAD - Smolyan. All used and repaired injection molds were analyzed over a period of one year.

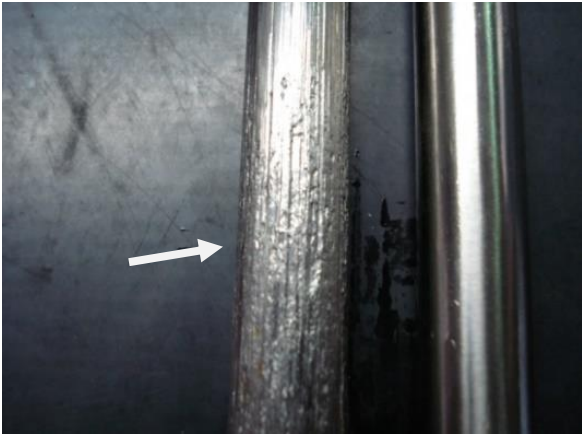


Fig.2.2. Destruction (scoring)



Fig.2.3. Corrosion wear

Fig. 2.2 shows mechanical wear (scoring) of an ejector due to sliding friction, accompanied by high temperature and insufficient hardness.

Fig. 2.3 illustrates corrosive wear due to the impact of chemically aggressive components in the polymer and the influence of the "diesel effect" when closing gas under high pressure.

Fig. 2.4 shows abrasive wear of the forming surface due to the abrasive action of the glass fibers in the material.

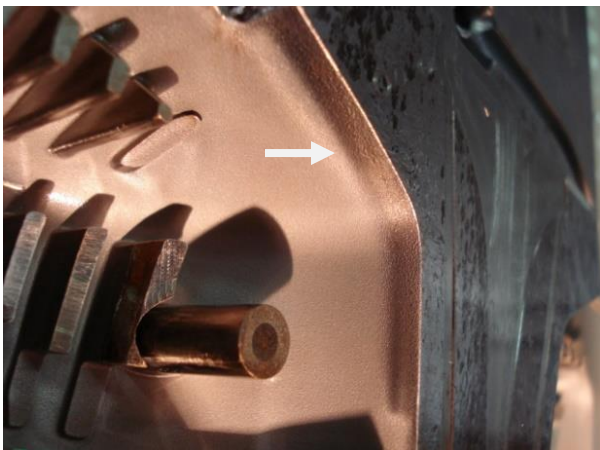


Fig.2.4. Abrasive wear



Fig.2.5. Material fatigue

Fig. 2.5 shows the chipping off of part of the mold due to material fatigue caused by cyclic bending and tensile loading, accompanied by sudden temperature changes.

2.2. Methods for increasing the wear resistance of injection molds

The following actions can be taken to increase the life of injection molds:

- simulation of the casting process and determination of factors affecting wear;
- optimization of the design and technology for making the tool and proper selection of tool materials;
- ensuring good gas removal from the molds;
- improving the drying of the material.

The resource of injection molds can be further increased through the following measures:

- increasing the hardness of the working surfaces of the tool;
- increasing the wear resistance of the working surfaces of the tool;

The most effective methods for performing these activities are hard coating methods. Recently, the most widely used methods have been physical (PVD) and chemical vapor deposition (CVD).

Conclusions from Chapter 2:

- The destruction of the metal surfaces of injection molds, abrasive and corrosive wear are caused mainly by fillers, flame retardants, reinforcing materials and other solid particles.
- Increasing the service life of injection molds can be achieved primarily by using modern technologies for applying hard coatings.
- For the correct choice of technological process for applying coatings, it is important to know the change in hardness of the tool steel after tempering.

Chapter 3. Materials, methodologies and tools for experimental research

3.1. Justification for the selection of specific materials and tools for research.

3.1.1. Selection of steel for testing

The choice of steel for the current studies is consistent with the following requirements:

- The price of the selected steel should not be too high.
- Possibilities are being considered for increasing the resource of both new and injection molds that are already manufactured and operating;
- As materials for active elements of new injection molds, it is appropriate to use stainless tool steels. The lower hardness could easily be compensated by applying a hard wear-resistant coating;
- The ability to apply hard wear-resistant coatings could significantly increase the life of both new and existing injection molds.

Based on the above requirements, Stavax ESR steel was selected for the study.

3.1.2. Selection of coverage for research

The choice of coating for the current studies is consistent with the following requirements:

- The steel selected for the study has anti-corrosion properties, therefore the choice of a wear-resistant coating should focus more on improving the tribological properties of the active elements, rather than on corrosion resistance;
- It would be good if the selected coating could be applied throughout the country.

Based on the above requirements, a gradient PVD coating Ti/TiN/TiCN was selected for research. The coating is characterized by high abrasion resistance, high hardness and impact toughness, very good adhesion to the substrate. The coating was applied at the Central Laboratory of Applied Physics at the Bulgarian Academy of Sciences - Plovdiv.

3.2. Methods for experimental studies of wear intensity and determination of mechanical and tribological characteristics of hard coatings

The study of the properties of coatings is carried out using modified methods for studying bulk materials, or with experimental studies for specific cases.

3.2.1. Methodology for experimental studies of the wear resistance of thin hard coatings using the volumetric method

To conduct wear resistance tests, a SIIP-1 stand [12] was used. A friction scheme was implemented using the “Ball on Flat Sliding Wear Test” method with a horizontal orientation of the tested surface (Fig. 3.2). During the test, the ball 2 (counter-body), which is fixedly fixed in a holder, rubs along a linear reciprocating moving sample (Reciprocation drive)

without the presence of lubricant and operating in air at room temperature. The ball is made of Al₂O₃ and has a diameter d = 3.0 mm. A load of 1.0; 2.0; 3.0; 4.0 and 5.0 N is applied to it.

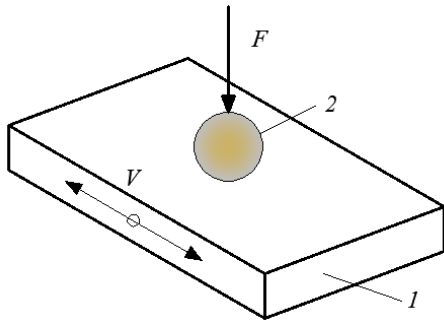


Fig. 3.2. Friction pattern according to the "Ball on Flat Sliding Wear Test" method
1 - sample; 2 – ball [78]

The wear channel on the surface has the shape shown in Fig. 3.3.

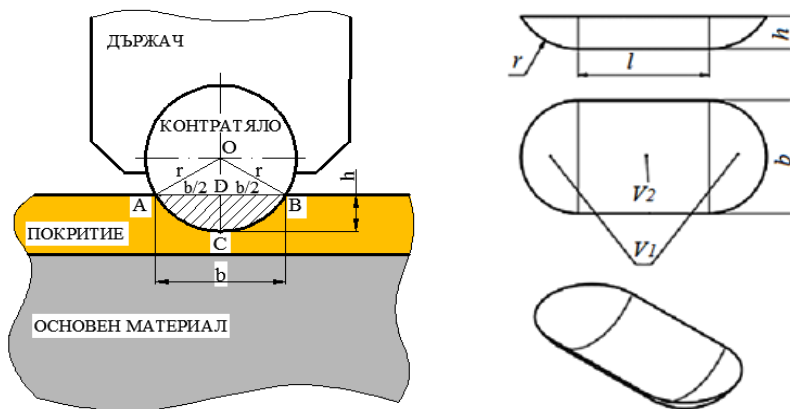


Fig. 3.3. Channel on the surface of the test specimen in a ball-on-plate tribological test
[3, 78]

A microscope is used to observe wear marks. It is assumed that the volume of the worn material is equal to the volume of the wear mark, when a sphere of known dimensions is reciprocated. The volume of the trace V is considered to be composed of two parts and is defined as [3, 4, 14]:

$$V = V_1 + V_2, \text{ mm}^3, \quad (3.1)$$

where V_1 – the volume of a segment of a sphere,
 V_2 – the volume of the straight part of the trace (a section of a cylinder).

$$V_1 = \frac{\pi}{3} \cdot h^2 (3r - h), \text{ mm}^3, \quad (3.2)$$

where h – the depth to which the counterbody has penetrated:

$$h = r - \sqrt{r^2 - \frac{b^2}{4}}, \text{ mm}, \quad (3.3)$$

where r – radius of the sphere, mm;
 b – track width, mm.

The volume of the straight part of the trace (a section of a cylinder) is determined by the relationship:

$$V_2 = S l_1, \text{ mm}^3, \quad (3.4)$$

where l_1 – length of the straight part of the track, mm;
 S – the cross-sectional area of the track, mm².

3.2.2. Methodology for determining the thickness of coatings by local abrasion with a rotating steel sphere

The methodology is based on the use of a device called a calo-tester. In the present study, the coating thickness was determined with a calo-tester – owned by the CLPF Plovdiv at the Bulgarian Academy of Sciences.

The wear is achieved by means of a hardened steel sphere with a diameter of Ø30 mm (30000 µm) sliding in the coated part of the specimen. The sphere is coated with an abrasive paste and rotates in place. As a result of the wear, circular (for planar surfaces) (Fig. 3.6) or elliptical (for cylindrical surfaces) indentations are obtained [29].

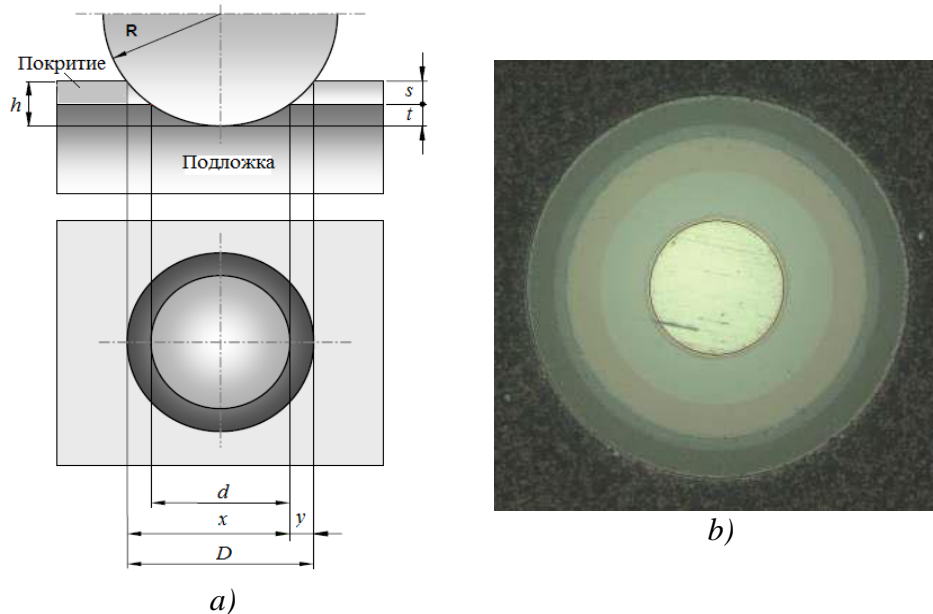


Fig. 3.6. Scheme of the wear imprint on planar surfaces a) [29] and spherical wear profile b) [72].

The layer thickness is defined as:

$$s = h - t, \quad (3.7)$$

where s – coating thickness, µm;
 h – total wear depth, µm;
 t – depth of the erased part of the pad, µm.

For thin layers, the wear depth is small compared to the radius of the sphere R . Therefore, the equation can be represented in the form [29]:

$$s = \frac{D^2 - d^2}{8R} \quad (3.8)$$

After substituting $D = x + y$ and $d = x - y$, the thickness is obtained:

$$s = \frac{xy}{2R} \quad (3.9)$$

The coating thickness is the average value determined by (3.8) or (3.9) for at least three attempts.

3.2.3. Methods for studying the physical-mechanical and tribological characteristics of thin-film hard coatings

The physical and mechanical properties of hard and superhard coatings are of significant practical importance, as they directly affect the service life of the products. The main mechanical indicator is hardness, but adhesion, wear resistance, modulus of elasticity, coefficient of friction, contact strength, etc. are also of great importance. The complex

assessment of these characteristics determines the applicability of a given coating, and currently there is no universal solution suitable for all cases.

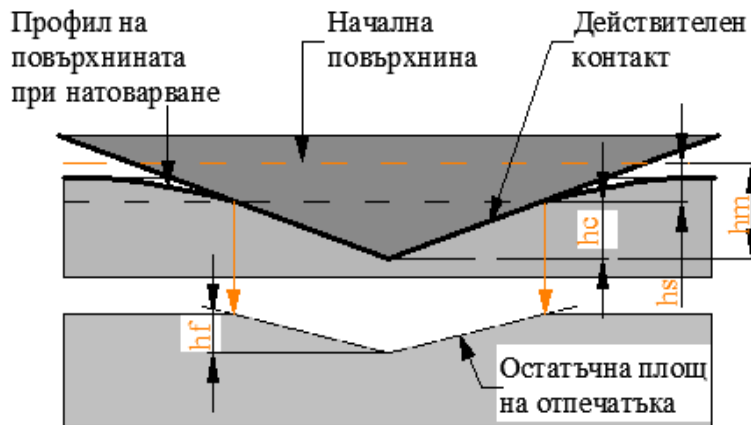


Fig. 3.7. Schematic of the nanoindentation process showing the residual area of the indentation after removal of the load (according to Oliver and Pharr)[63].

In this work, a Compact Platform CPX (MHT/NTN) nanohardness tester from the company CSM Instruments, installed at the Central Laboratory of Applied Physics - Plovdiv, was used.

A schematic diagram of the nanoindentation process, showing the decrease in penetration depth after removal of the load, is shown in Fig. 3.7.

To conduct the coverage studies, a Berkovich type indenter is used.

3.2.4. Methodology for determining the adhesion between the coating and the base metal (Scratch-test)

A schematic diagram of the operation is shown in Fig. 3.10. A movable table, on which the sample with the coating is fixed, moves at a constant linear speed, during which the diamond-tipped needle (indenter) in contact with the coating scratches and leaves a mark on it. During the translational movement of the table, the load on the needle gradually increases. The tip of the needle has an angle $\alpha = 120^\circ$ and a radius of curvature of $200 \mu\text{m}$. The speed of movement of the movable table is $v = 10 \text{ mm/min}$, and the usually traveled distance is $s = 3 \text{ mm}$. The load F increases from 0 to 30 N with an intensity $dF/ds = 10 \text{ N/mm}$.



Fig.3.10. How the scratch test works [127, 136]

For the determination of cohesion and the adhesion was tested using the Scratch test method, conducted using a Compact Platform CPX (MHT/NHT) CSM Instruments device at the Central Laboratory of Applied Physics - Plovdiv.

3.2.5. Methodology for studying surfaces using Atomic-Force Microscopy (AFM)

An atomic-force microscope (AFM) model XE-100, manufactured by Park Systems, was used to conduct the experiments., owned by the University of Craiova, Romania.

CONCLUSIONS FROM CHAPTER 3

- A set of methodologies for determining the tribological parameters of thin hard coatings is presented.
- Traditional hardness determination methods are not suitable for determining the hardness of hard and superhard coatings.
- The applied AFM methodology in non-contact mode allows reliable and detailed examination of surfaces with nanometric resolution without damaging the sample.

Chapter 4. Simulation of the injection molding process. Factors affecting wear and opportunities for tool design optimization

For the purposes of this work, Moldex 3D software was used to simulate the molding process for a housing part for a pressure sensor. Based on the results of this simulation, an injection mold for the product in Fig. 4.1 was designed and manufactured.

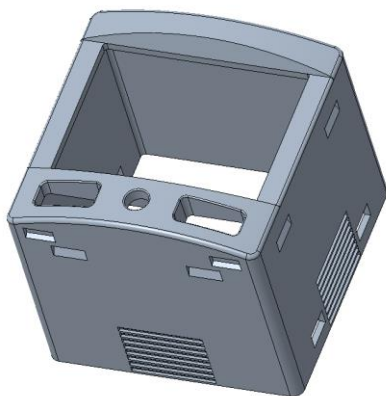


Fig.4.1. Housing part for pressure sensor

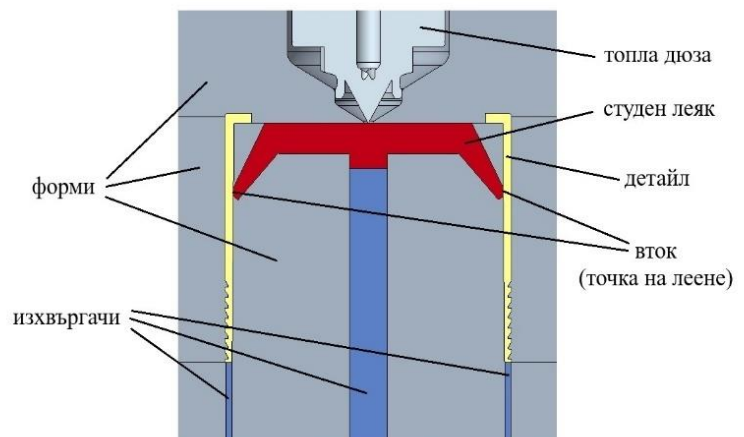


Fig.4.2. Two-sprue molding scheme

In order to achieve a more balanced filling of the molds and eliminate unwanted deformations of the cold sprue leading to its retention in the tool during ejection, a molding scheme with two gates (casting points) was chosen, shown in Fig. 4.2.

Due to the planned annual volume of parts required for production, the tool has 2 cavities, i.e. 2 parts will be produced simultaneously for one production cycle. Further increasing the number of cavities is not advisable, due to the need to place 4 movable molds (sliders) for each cavity (Fig. 4.3). These movable molds serve to form ribs and technological holes in the side walls of the product and to release the part when opening the injection mold before its ejection after cooling.

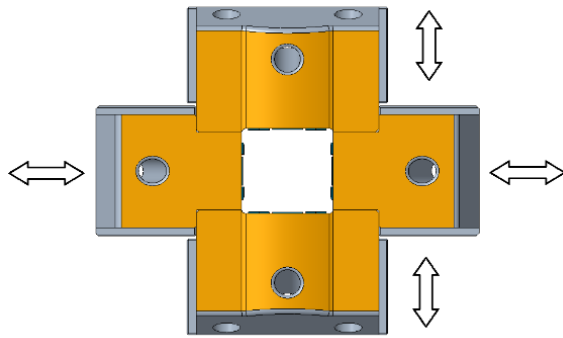


Fig.4.3. Movable sliders of the injection mold cavity

Since the injection molding machine has a single melt injection point, filling two or more cavities simultaneously requires dividing the melt flow into a corresponding number of equal parts. For this purpose, a hot runner system is suitable.

- **Analysis of the results obtained**

After completing the calculations, the Moldex 3D software presented the following process simulation results:

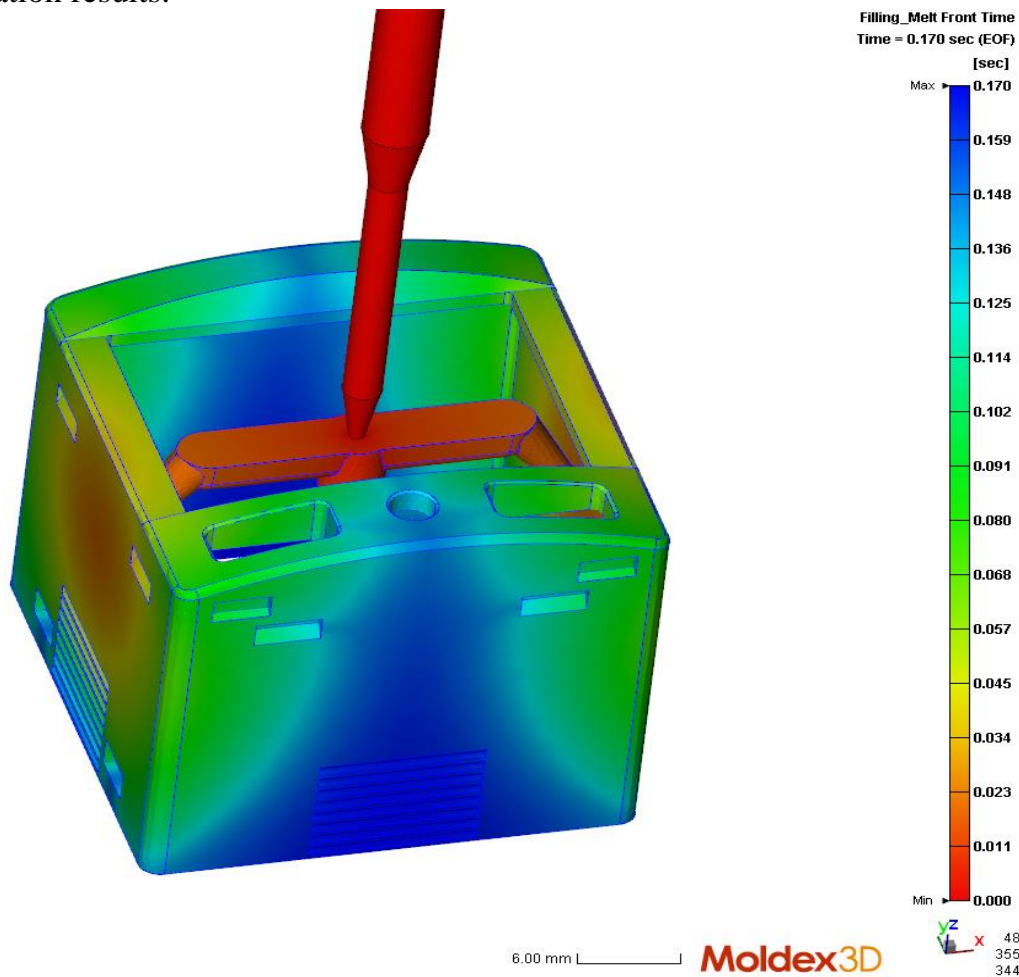


Fig.4.10. Filling time

Time to fill the mold (Fig.4.10). Different colors represent the time it takes for the melt to reach the corresponding section of the part. The color scale is located on the right of the image.

It is visible that the areas colored in dark blue are the last zone to which the melt reaches. Usually in these areas the air trapped in the mold is concentrated, which is pushed out by the melt in the filling stage, as well as the gases released from the polymer during injection molding. This is a prerequisite for the appearance of a defect in the manufactured product due

to the diesel effect. This is clearly confirmed in the following figure, where the zones in which air is trapped are visualized (Fig.4.11).

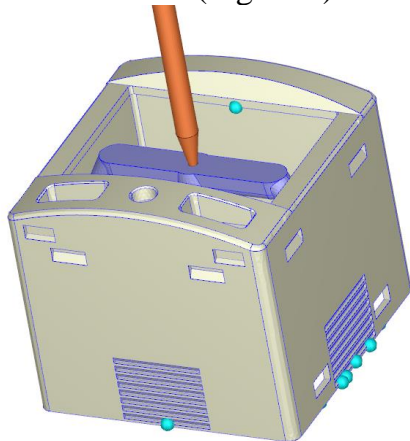


Fig.4.11. Zones of concentration of air trapped in the mold and gases released from the melt

Blue spheres indicate the places where compressed gases from the melt accumulate. To eliminate potential problems with the quality of the manufactured parts and to remove the gases from the mold, it is necessary to provide ventilation channels in these areas. Installing a replaceable element with increased anti-corrosion properties would lead to improved wear resistance and reparability of the injection mold.

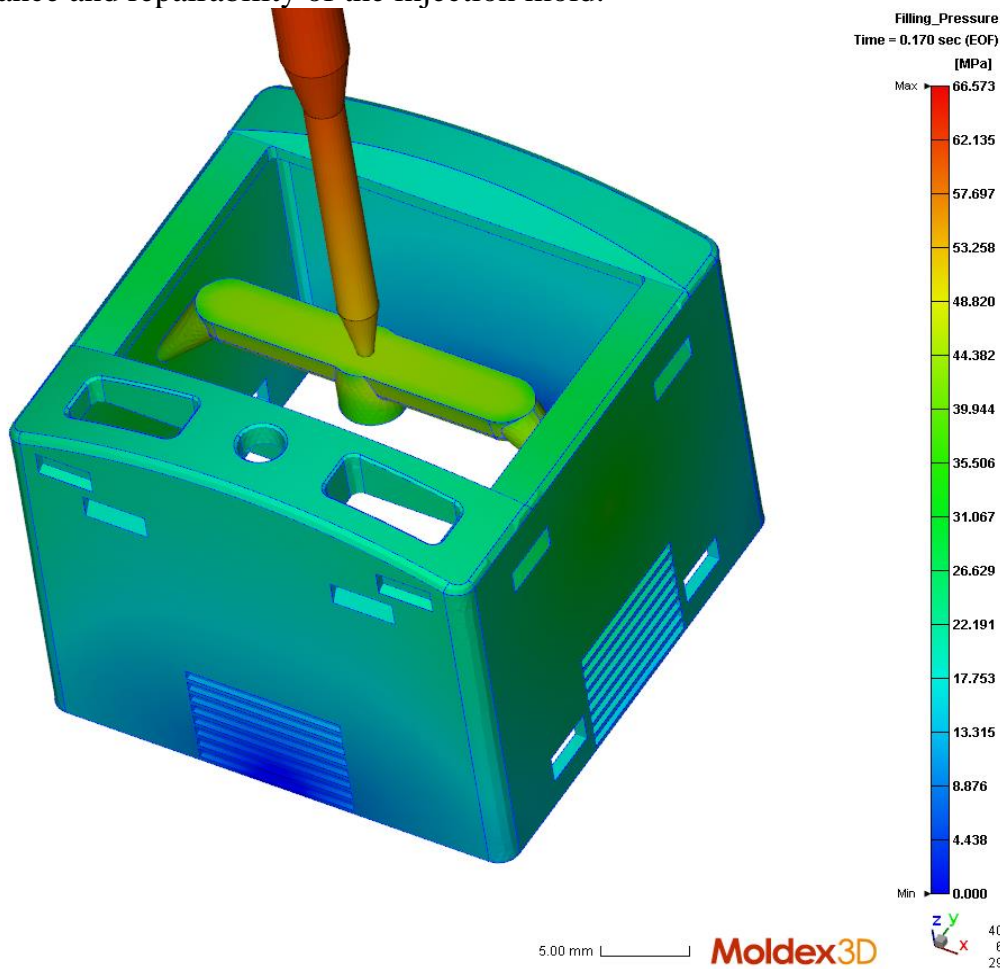
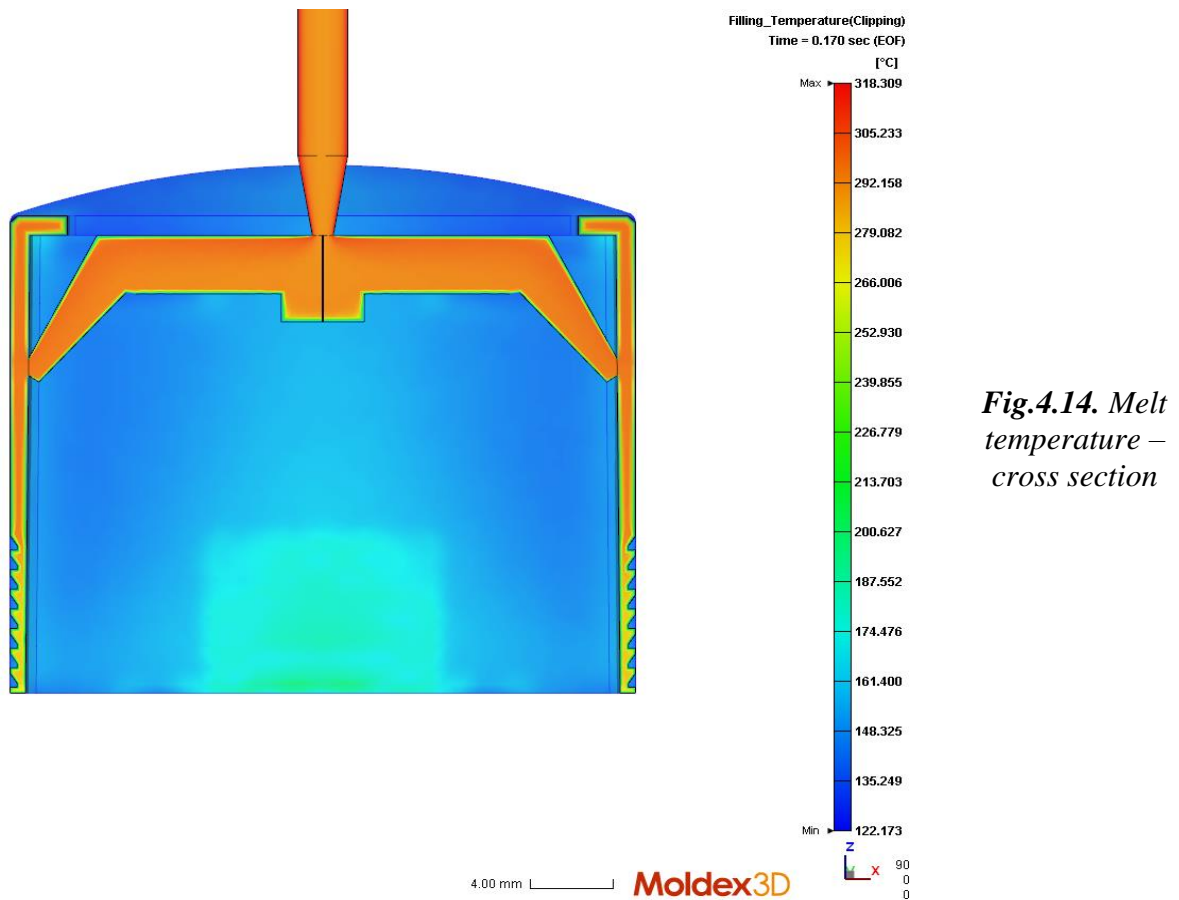


Fig.4.12. Melt pressure

The melt pressure is presented in Fig. 4.12.

From a design point of view, the melt pressure in certain zones is an important condition for the performance of the injection mold [76].

A cross-section of the part shows the temperature distribution in the melt volume (Fig. 4.14)



Of particular importance for the wear of the working surfaces of injection molds is the presence of glass or carbon fibers in the polymer and their orientation during the molding process. In most cases, they are oriented in the direction of the melt flow. In the presence of narrow sections, sharp changes of direction and other obstacles, the fibers hit the walls with their ends and lead to increased abrasive wear compared to other areas.

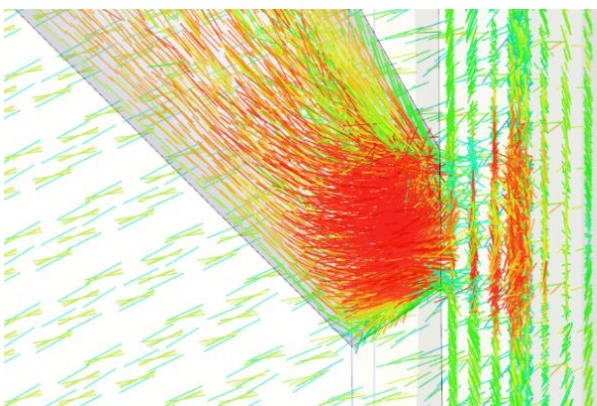


Fig.4.17. Orientation of glass fibers at injection point No.1

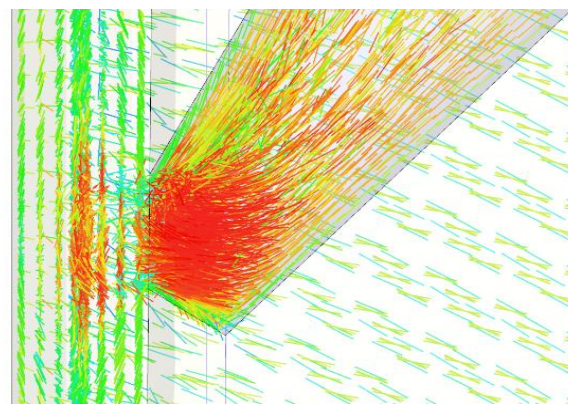


Fig.4.18. Orientation of glass fibers at injection point No.2

In Fig. 4.17 and 4.18, cross-sections of the injection points are presented. The change in the direction of movement of the glass fibers in these areas is clearly visible. During the movement of the melt, the fibers hit the ends of the thin wall in the transition zone between the conical hole on the gate and the mold cavity, as a result of which it is expected that there will be an increased intensity of wear in this area during the operation.

- **Calculating the required mold clamping force**

Based on the minimum injection pressure for filling the injection mold and the packing pressure obtained from the simulation, the required clamping force can also be determined.

The minimum clamping force of the two halves of the injection mold is determined by the following expression:

$$F_{\min 1} = \sum_1^n p * A, [112], \quad (4.1)$$

where

$F_{\min 1}$ – minimum clamping force, N;

n – the number of segments into which the total area is divided;

p – melt pressure in the mold, Pa;

A – the area of each segment as a projection of the surface of the product onto the parting plane, m².

The data for the designed area of the part and the sprue are taken directly from the software, without having to make arithmetic calculations (Fig. 4.23).

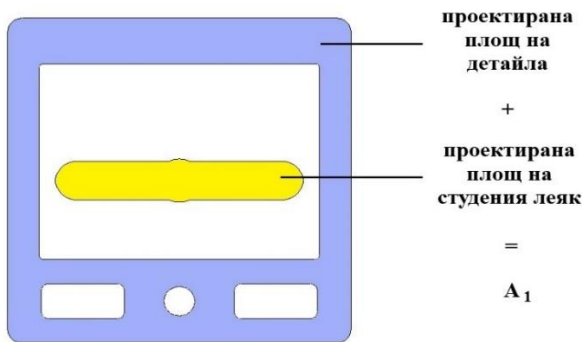


Fig.4.23. Projection of the total area A_1 of the part and the sprue onto the parting plane

The input data for calculating the minimum clamping force are:

- $p = 66573000$ Pa – maximum injection pressure from the simulation;
- $A_1 = 0.000480817$ m² – the calculated designed area of the part and the cold runner for one cavity.

The minimum clamping force for 2 cavity will be:

$$F_{\min 1} = 2 * 66573000 * 0,000480817$$

$$F_{\min 1} = 64\ 018,86\ N$$

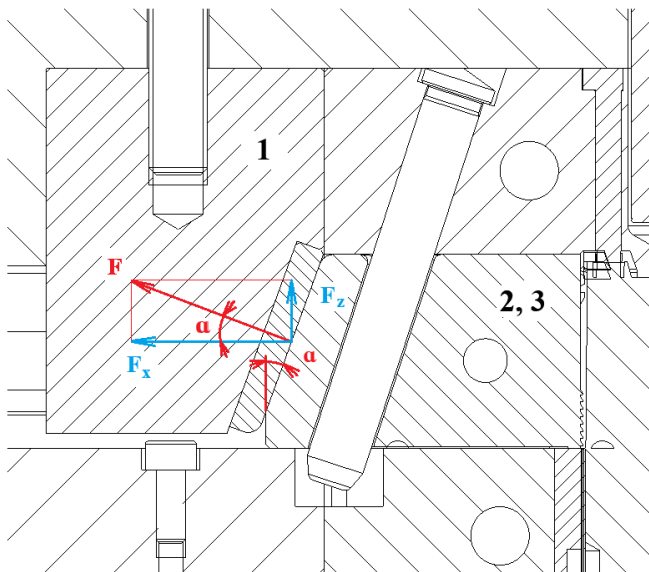


Fig.4.24. Forces caused by the pressure of the melt on the wedges for pressing the sliders

The above calculations must also take into account the presence of sliding elements in the injection mold - 2 and 3, which are pressed by a wedge - 1 (Fig. 4.24). When injecting the polymer into the mold, the pressure of the melt in the cavity is distributed evenly on all sides. The force generated by the melt presses the slider and the pressing wedge of the slider. Since the area is inclined, part of the force is redirected to the parting plane of the mold and tends to open the two halves of the tool. This fact has an additional impact on the calculation of the total closing force.

The magnitude of the force F_Z will be:

$$F_Z = F_X \cdot \tan \alpha \quad (4.2)$$

There are 4 sliders for shaping each part in total, with the oppositely located sliders being the same, i.e. we have 2 types of sliders, two of each type for each part. The projections of the sliders in a plane perpendicular to both the dividing plane and the direction of their movement are shown in Fig. 4.25. The areas are respectively designated by A_2 and A_3 , and the values for the surface of the projections are again taken from the 3D design software and are: $A_2 = 771.248 \text{ mm}^2$, $A_3 = 650.529 \text{ mm}^2$

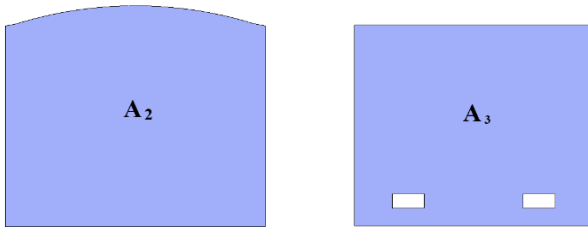


Fig.4.25. Effective areas A_2 and A_3 over which the force transmitted by the melt is distributed

The expression for calculating the force F_Z for both cavity will look like this:

$$F_Z = F_X \cdot \tan \alpha = p \cdot 4(A_2 + A_3) \cdot \tan 20^\circ$$

$$F_Z = 66,573 \cdot 10^6 \cdot 4(771,248 \cdot 10^{-6} + 650,529 \cdot 10^{-6}) \cdot 0,364$$

$$F_Z = 137\,813,25 \text{ N}$$

From the calculations made, it is evident that in this particular case, the pressure exerted by the melt on the sliders generates a force counteracting the clamping force of the tool more than twice as large as that generated in the parting plane.

The total minimum mold clamping force is:

$$F_{min} = F_{min1} + F_Z \quad (4.3)$$

$$F_{min} = 64\,018,86 + 137\,813,25$$

$$F_{min} = 201\,832,11 \text{ N} = 201.83 \text{ kN}$$

Due to manufacturing deviations, friction between the wedges and sliders during closing, possible fluctuations in the working process, elastic deformations of the mold plates and other reasons, the resulting value is usually increased by about 20%.

CONCLUSIONS FROM CHAPTER 4:

1. Computer simulation provides data on areas of gas accumulation and uneven cooling, which allows early correction of the injection mold design and taking actions to reduce wear.

2. The simulation results show that the presence of narrowed sections and obstacles in the path of the melt can lead to a local excess of the temperature of the liquid polymer above the upper limit of its operating range. This can activate harmful processes leading to corrosive wear of the working surfaces of the injection mold.

3. The formation of acidic products at high temperatures necessitates the use of resistant coatings or materials for the active parts of tool.

4. The simulation results indicate the probability of intense wear of the working surfaces of the injection mold at the injection points.

5. The presence of glass fibers (GF30) in the polymer increases the abrasive wear of the molds – especially in areas with sharp changes in flow direction.

6. The calculation of the minimum clamping force is an important parameter necessary for the strength calculation of the forces acting on the injection mold and the prevention of unwanted deformations. Computer simulation is able to provide indicative data on the melt pressures, from which the minimum clamping force can be calculated.

Chapter 5. Experimental studies of wear resistance, topography of hard coating and laser welded layers on Stavax ESR steel

5.1. Analysis of mold wear in the molding zone

An analysis of the wear of the active parts of an injection mold made of STAVAX ESR steel was performed in the areas of melt flow into the cavity (the injection points). The measured hardness of both molds is 52 HRC. A simulation of the molding process of the specific injection mold is presented in Chapter 4. Measurements were made of the dimensions of the melt injection holes after 213,000 working cycles. The dimensions of the holes in the production of both molds with the tolerances are presented (Fig.5.1).

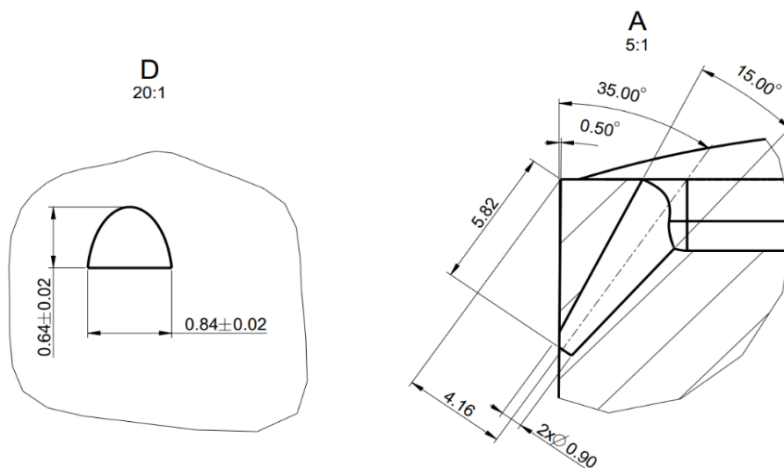


Fig.5.1. Drawing of the melt injection holes

The condition of the measured holes can be seen in Fig. 5.2 – 5.3.

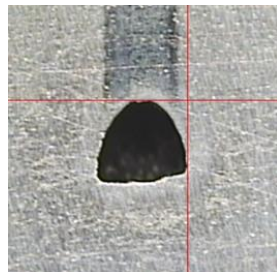
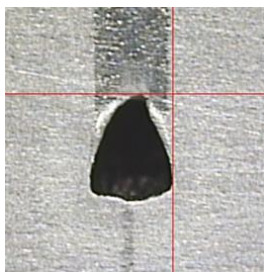


Fig.5.2. Injection points 1 (left) and 2 (right) of cavity No.1



Fig.5.3. Injection points 1 (left) and 2 (right) of cavity No.2

The measurement results of the four melt injection points after continuous operation are presented in table 10. The measurements were performed with a TESAVISIO - 300 microscope with a magnification of 20 to 130 times and a resolution of 0.001 mm.

Results of measuring the melt injection holes after 213,000 production cycles **Table 10**

Nominal diameter, mm	point 1, cavity №1, mm	point 2, cavity №1, mm	point 1, cavity №2, mm	point 2, cavity №2, mm
0.840	0.850	0.930	0.913	0.880
0.640	1,105	0.880	0.866	0.924

Considering the presence of 30% glass fibers in the polymer used, as well as the number of working cycles of the tool, it can be assumed that wear is minimal. Most likely, this is due to:

- the use of corrosion-resistant Stavax ESR steel to make the active parts;
- suitable angle for ejecting the cold sprue.

5.2. Study of the wear resistance of Ti/TiN/TiCN hard coating deposited on STAVAX ESR steel

5.2.1. Sample preparation

The test specimens are made of tool steel, widely used for the production of active parts for injection molds – Stavax ESR (AISI 420 modified). The chemical composition of the specific specimens, provided by the steel manufacturer, is presented in Table 11:

Chemical composition of Stavax ESR for the tested samples **Table 11**

	C	Yes	Mn	Cr	V	P	S
%	0.40	0.91	0.45	13.4	0.28	0.021	0.0004

The samples have the shape of a rectangular parallelepiped with dimensions LxBxH, mm, (Fig.5.4). The following groups of samples were prepared (Table 12).

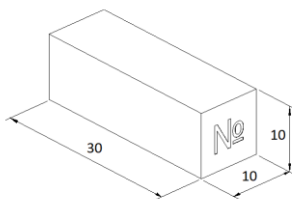


Fig.5.4. Research sample

Types of samples **Table 12**

No.	Processing
A (1-3)	Unhardened, ground
B (4-8)	Hardened, ground
C (9-12)	Tempered, polished
D (13-15)	Tempered, polished, ref. specimen

The heat treatment of the samples was carried out in a chamber furnace with a temperature reaching 1100 °C - brand SNOL - M, Balchik.

Tested samples **Table 13**

Sample		Type of coating	Hardness before coating	Roughness of the sample before coating Ra, μm	Roughness of the coated sample Ra, μm
A	1	Unhardened, ground, coated	191 HB	0.29	0.30
	2			0.24	0.24
	3			0.25	0.30
B	4	Hardened, ground, coated	53 HRC	0.18	0.22
	5			0.19	0.20
	6			0.18	0.20
	7			0.19	0.20
C	8	Tempered, polished, coated	53 HRC	0.17	0.18
	9			0.04	0.10
	10			0.03	0.10
	11			0.03	0.10
	12			0.04	0.10

D	13	Tempered, polished, ref. specimen	-	53 HRC	0.04	-
	14				0.04	-
	15				0.04	-

The hardness of the hardened samples is 53 HRC. The hardness was measured with a ZIP hardness tester, Model TK-2M. The roughness of the samples was measured with a Zeiss – Handysurf E-30A roughness tester [101]. Data on the measured hardness and roughness of the tested samples are given in Table 13.

A Ti/TiN/TiCN coating was applied to the prepared samples by electric arc evaporation in a high-vacuum PLATIT π 80+ (Platit Advanced Coating Systems) installation, owned by the Central Laboratory of Applied Physics - Plovdiv at the Bulgarian Academy of Sciences.

5.2.2. Conditions for conducting experimental studies of wear resistance using the volumetric method of thin hard coatings

The coating thickness was measured using a calo-tester (a special design of the Central Laboratory of Applied Physics, Bulgarian Academy of Sciences) using a 30 mm ball of bearing steel.

Nano-hardness and elastic modulus were investigated with the Compact Platform CPX (MHT/NHT) (CSM Instruments). A Berkovich type diamond indenter was used. Data processing was performed using the Oliver-Pharr method (software embedded in the equipment). Four load values were used: 10, 20, 50 and 100 mN, with 3 measurements performed with each of these values, and the results averaged.

Adhesion was tested using a Micro Scratch Tester (MST) module, which is part of the aforementioned equipment. A Rockwell diamond indenter with a 200 μ m tip rounding and a sliding distance of 3 mm was used.

Initially, some of the mechanical parameters related to wear resistance were investigated. The hardness of the unhardened samples was 191 HB, and of the hardened samples - 53 HRC. The measured thickness of the coating was 2.00 μ m, and it had a copper-red color. The cross-section looks clear, without traces of destruction, which suggests low internal stress in the coating.

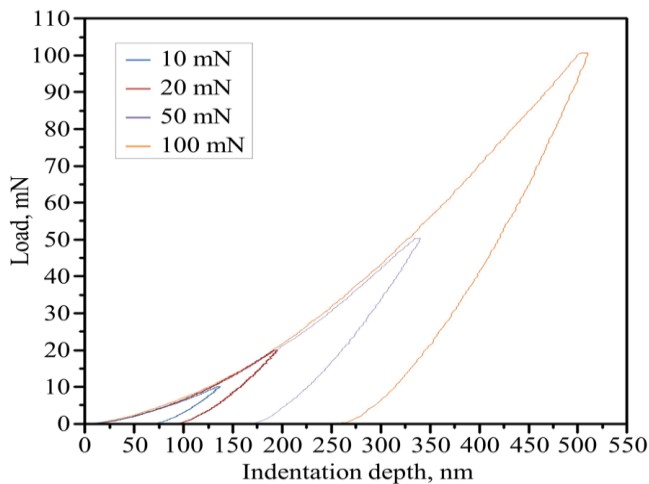


Fig.5.6. Loading and unloading curves at different loads

The determination of nanohardness was carried out at indenter loads of 10, 20, 50 and 100 mN. The resulting curves are depicted in Fig. 5.6.

At a load of 20 mN, a penetration depth of 193 nm was achieved, with a hardness of 35 GPa on average. This was accompanied by a Young's modulus of 434.0 GPa on average. The loading and unloading curves cover a wide range, suggesting that the coating is relatively strong [84].

During the scratch test, no adhesion or cohesion disruptions were observed up to a maximum needle load of 30 N. The measured friction coefficient has a constant value of about 0.15.

The wear resistance of the coating was assessed with a SIIP-1 stand at the Faculty of Physics and Technology of the Paisii Hilendarski University.

The experimental studies were conducted using a friction scheme using the “Ball on flat sliding wear test” method with a horizontal orientation of the tested surface. A mineral ceramic ball of Al₂O₃ with a diameter $d = 3.0$ mm, fixed in a holder, is used as a counterbody. The counterbody is rubbed linearly, in a pattern performing reciprocating movements with a length of 11 mm. There is no lubricant. The installation operates at a temperature of 20° C. A load of 1, 2, 3, 4 and 5N is applied to the counterbody. The width of the grooves was measured with a microscope TESAVISIO - 300 with a magnification of 20 to 130 times and a resolution of 0.001 mm. The average value of the width of the wear mark (track) is determined:

$$b_{cp} = \frac{1}{n} \sum_i^n b_i, \text{ mm} \quad (5.1)$$

The wear rate I_w is determined by the dependence:

$$I_w = \frac{V}{F.L}, \text{ mm}^3/\text{Nm} , \quad (5.2)$$

where: V – the volume of the amount of material removed (the track), mm³;

F – the normal load, N;

L – the distance traveled by the sample, relative to the counterbody, m.

The volume of the track is determined using the methodology described in item 3.2.1.

5.2.3. Study of the influence of normal force on wear intensity

Experimental studies on the influence of normal force on the wear rate of a Ti/TiN/TiCN multilayer coating were conducted at the following constant tribosystem parameters:

- Average sliding speed $V_{av} = 10$ mm/s;
- Gliding distance traveled $L = 50$ m.

Volume of wear marks as a function of load

Table 14

Volume of the track as a function of the load $V=f(F)$, $v=10\text{mm/s}=\text{const}$, $L=50\text{m}=\text{const}$				
	Load, F , N	Ti-TiN-TiCN-Stavax ESR_A .10 ⁻⁶ , mm ³	Ti-TiN-TiCN-Stavax ESR_B .10 ⁻⁶ , mm ³	Ti-TiN-TiCN-Stavax ESR_C .10 ⁻⁶ , mm ³
Track 1	1	814,044	596,299	214,064
Track 2	2	1095,596	805.161	215,896
Track 3	3	1334.027	1042.121	269,406
Track 4	4	1397.017	1377.916	286,809
Track 5	5	1583.903	1468.136	377,097

Summary data on the values of the wear track volumes as a function of the load $V=f(F)$ at the corresponding loads are given in Table 14.

Fig. 5.8 presents the graphical dependence of the volumes of wear track for the coated samples as a function of the load $V=f(F)$.

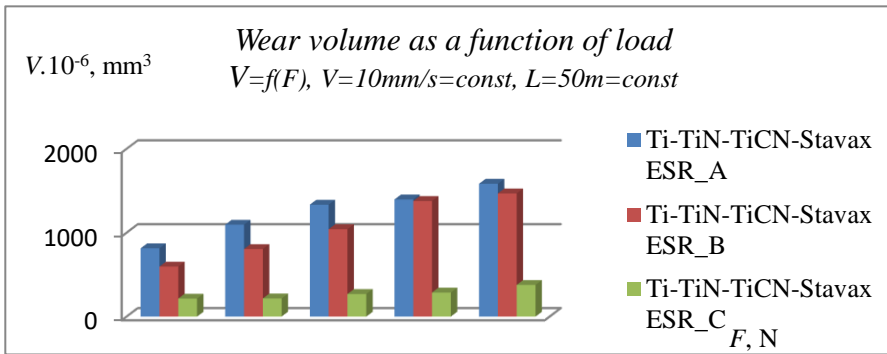


Fig.5.8. Wear volume as a function of load

Data on the wear rate as a function of the load $I_w=f(F)$ at the corresponding loads are given in Table 15.

Wear rate as a function of load

Table 15

Wear rate as a function of load $I_w=f(F)$, $v=10\text{mm/s}=\text{const}$, $L=50\text{m}=\text{const}$				
	Load, F , N	Ti-TiN-TiCN-Stavax ESR_A .10 ⁻⁶ , mm ³ /N m	Ti-TiN-TiCN-Stavax ESR_B .10 ⁻⁶ , mm ³ /N m	Ti-TiN-TiCN-Stavax ESR_C .10 ⁻⁶ , mm ³ /N m
Track 1	1	16,281	11,926	4.281
Track 2	2	10,956	8.052	2.159
Track 3	3	8.894	6.947	1,796
Track 4	4	6.985	6.889	1.434
Track 5	5	6.675	5.874	1.508

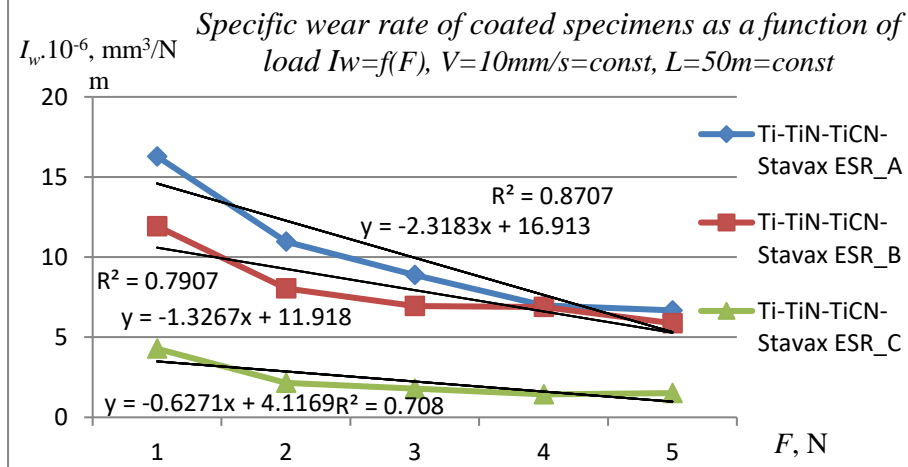


Fig.5.9. Specific wear rate of coated specimens as a function of load

Table 16 provides summarized data on the values of the volumes of the wear marks of the polished samples as a function of the load $V=f(F)$ at the corresponding loads.

Volume of wear marks as a function of load

Table 16

Volume of the track as a function of the load $V=f(F)$, $V=10\text{mm/s}=\text{const}$, $L=50\text{m}=\text{const}$			
	Load F , N	Ti-TiN-TiCN-Stavax ESR_C .10 ⁻⁶ , mm ³	Stavax ESR_D - ref. specimen .10 ⁻⁶ , mm ³
Track 1	1	214,064	1801.93
Track 2	2	215,896	12287.04
Track 3	3	269,406	32816.47
Track 4	4	286,809	87265.47
Track 5	5	377,097	159023.9

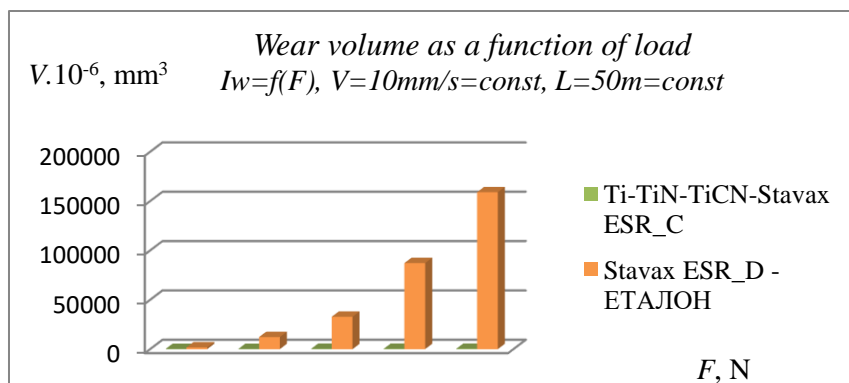


Fig.5.10. Wear track volume of polished coated and reference (uncoated) samples as a function of load

The graphical dependences of the volumes of wear marks when testing the coated samples and the reference (uncoated) samples under the corresponding regimes are shown in Fig. 5.10.

Table 17 summarizes the data on the wear rate values of the polished (coated and uncoated) samples as a function of the load $I_w=f(F)$.

Wear rate as a function of load on hardened, polished coated and reference (uncoated) specimens
Table 17

<i>Wear rate as a function of load $I_w=f(F), V=10\text{mm/s}=\text{const}, L=50\text{m}=\text{const}$</i>			
	Load, F, N	Ti-TiN-TiCN-Stavax ESR_C	Stavax ESR_D - ref. specimen
		$\cdot 10^{-6}, \text{mm}^3 / \text{N m}$	$\cdot 10^{-6}, \text{mm}^3 / \text{N m}$
Track 1	1	4.281	36.03859
Track 2	2	2.159	122.8704
Track 3	3	1.796	218.7765
Track 4	4	1.434	436.3274
Track 5	5	1.508	636.0955

The graphical dependences of the wear rate of the polished (coated and uncoated) samples as a function of the load $I_w=f(F)$ are presented in Fig. 5.11.

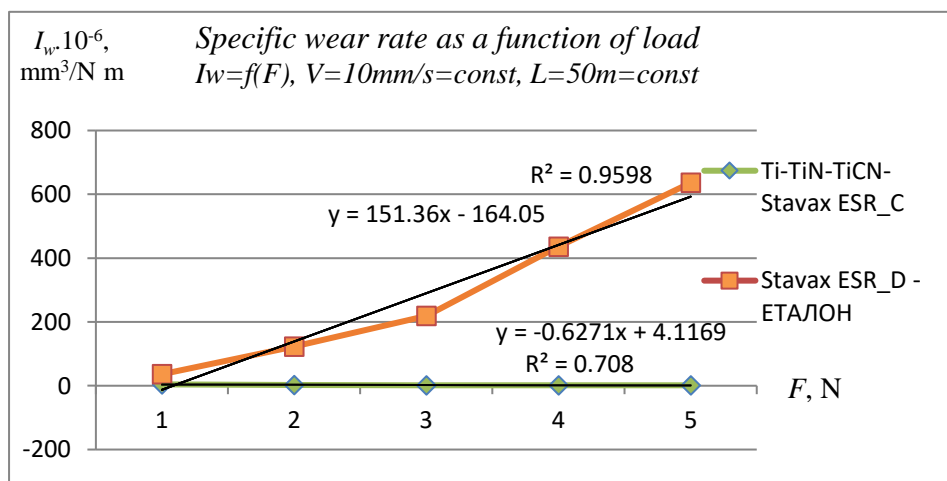


Fig.5.11. Specific wear rate as a function of load

5.2.4. Analysis and conclusions

- In the polished samples, an increase in roughness was observed after coating, while in the ground samples, it was preserved compared to the uncoated ones. This is probably due to the presence of microdroplets (non-ionized metal particles), which is characteristic of the process [59];

- The volume criterion is used to determine wear. The volume of the trace increases with increasing load. The specific wear rate of the coated specimens decreases with increasing load. This type of coating, deposited on Stavax ESR steel, is suitable for products operating under high loads.

- The roughness of the samples has a significant impact on the intensity of coating wear. The coating applied to a hardened and polished sample has the smallest wear volume compared to a hardened ground and unhardened ground sample (Fig. 5.8).

- The obtained wear rate values are low, and are close to the lower limit of the results shown in most similar studies [27, 84], which further determines the coating suitable for application on injection molds.

- The wear rate of a multi-layer Ti/TiN/TiCN coating applied to a hardened Stavax ESR steel substrate with polished surfaces is on average 130 times less than that of an uncoated one.

5.3. Investigation of the topography of a Ti/TiN/TiCN hard coating deposited on STAVAX ESR steel

The purpose of the study is to determine the quality of the surface layer after coating, as well as the presence of any possible defects.

The surface layer of mirror-polished samples of Stavax ESR steel, coated with a hard wear-resistant coating of Ti/TiN/TiCN, was investigated using an atomic force microscope Park Systems, model XE 100 at the University of Craiova - Romania. For the purposes of the study, a non-contact method was used. The dimensions of the scanned areas are 45 μm x 45 μm . Three areas of each sample were scanned.

5.3.1. Research results

Images of scanned sections of polished samples with Ti/TiN/TiCN coating are shown in Fig. 5.13 – 5.15. The difference in scales in the coating plane and in height should be taken into account.

Conical formations protruding above the surface of the planar layer of the coating are observed, as well as cavities extending into the coated area.

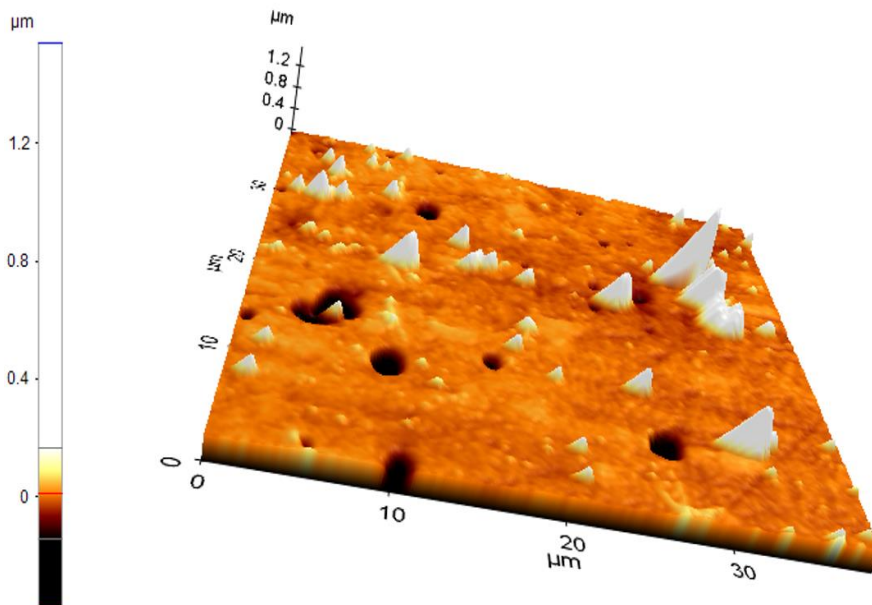


Fig.5.13. AFM image of the surface of a mirror-polished sample No. 10 of STAVAX ESR steel with a hard wear-resistant coating of Ti/TiN/TiCN

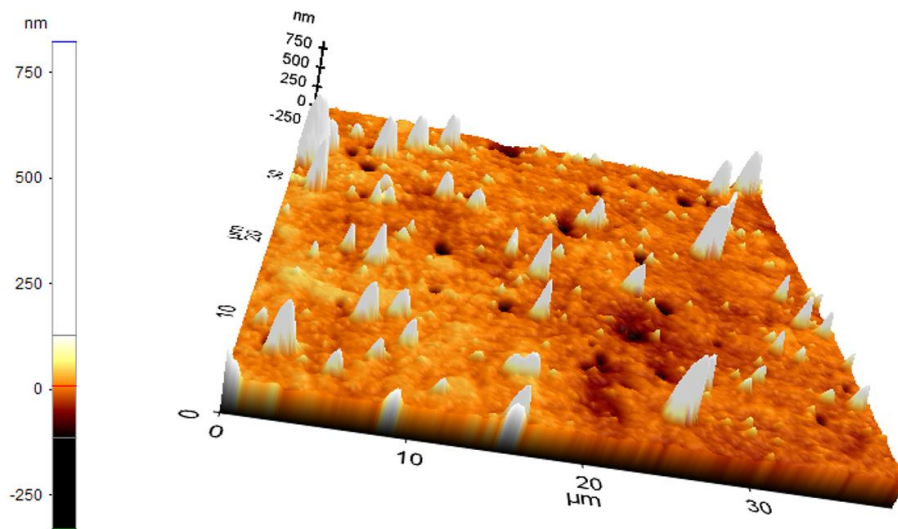


Fig.5.14. AFM image of the surface of mirror-polished sample No. 11 of STAVAX ESR steel with a hard wear-resistant coating of Ti/TiN/TiCN

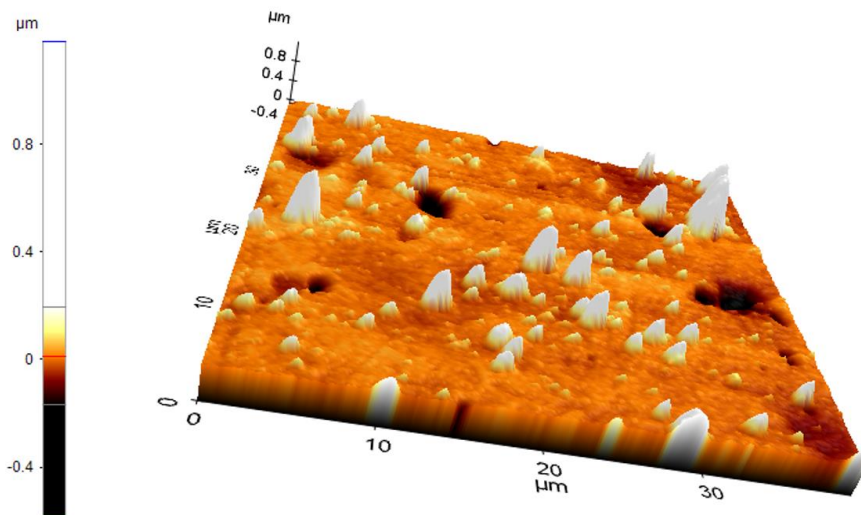


Fig.5.15. AFM image of the surface of a mirror-polished sample No. 12 of STAVAX ESR steel with a hard wear-resistant coating of Ti/TiN/TiCN

Analysis and conclusions

The origin of the protrusions is most likely due to:

- Accumulations of Ti ions (droplets) on the tips of the microroughness's on the surface in the initial stage of coating formation, invariably accompanying the arc deposition process;
- Etching tips coated with a coating. Since the tips concentrate positive ions towards themselves, and these are the metal ions that create the coating, there is a possibility that the coating will be dominant there.

Most likely, the depressions are due to similar conical formations mentioned above, which, as a result of cleaning the sample before testing, have separated from the surface. The reason for their detachment is poor adhesion to the coating. From the measurements of the profile in the intersecting planes (Fig.5.19) it is evident that the depth of the depression in the studied areas does not exceed 600 nm, which gives reason to assume that this defect will not have a significant impact on the quality of the coating.

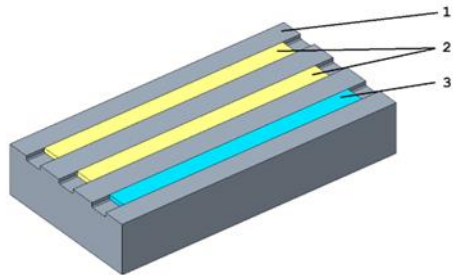
5.4. Investigation of the properties of laser welded steel layers on a substrate – STAVAX ESR steel

In most cases, the wear is localized to the most stressed areas. Restoring these areas would significantly extend the life of the injection mold. A suitable method for this is laser welding.

The present study aims to compare the roughness and hardness of laser-welded layers with two types of filler material under three different types of finishing regarding the substrate used. STAVAX ESR steel, which is commonly used in injection moulding due to its good physical and mechanical properties, was chosen as the substrate material.

5.4.1. Sample preparation

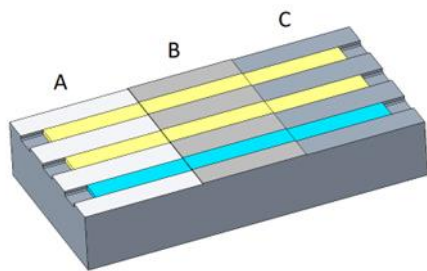
A ground specimen (1) made of STAVAX ESR steel with preformed grooves hardened to a hardness of 50.5 HRC was prepared for the study (Fig.5.21). The channels were subsequently filled with laser welded layers of two different additive materials, STAVAX ESR steel additive material – SDL STA (2) and SDL 14 additive material (3).



- 1- Stavax ESR
- 2- SDLSTA
- 3- SDL 14

Fig.5.21. Arrangement of laser welded layers

The thickness of the laser-welded layer after cleaning by grinding the weld seams is 0.5mm. Additional processing was performed so that 3 zones could be distinguished (Fig.5.22):



- A – mirror polished area;
- B – grinded area;
- C – zone eroded with EDM with grain size 24 – 27, VDI 3400.

Fig.5.22. Position of the areas with finished processing

The laser welding was performed on an AlphaLaser AL-T 500 installation, with a filler material with a diameter of 0.5 mm.

The roughness of the obtained surfaces was studied on an Atomic Force Microscope Park Systems, model XE 100 at the University of Craiova. For the purposes of the study, a non-contact method was used. The dimensions of the scanned areas were 45 μm x 45 μm. 3 areas of each type of surface were scanned, after which the obtained results were averaged.

5.4.2. Testing the hardness and roughness of the welded layers and comparing the results with the base material

The results of the measured hardness are shown in Table 20.

Measured hardness of the different layers in the polished area Table 20

<i>Layer</i>	<i>Value</i>	<i>Units</i>
STAVAX ESR	50.5	HRC
SDL STA	47.7	HRC
SDL 14	19.7	HRC

The results of the measured roughness are shown in Tables 21 - 23. It is evident from the data that the values from the measurement of the roughness of the welded layers are very close to the roughness of the base material for all three types of finishing treatments.

Measured roughness of the different layers of mirror-polished surfaces **Table 21**

<i>Layer</i>	<i>Surface condition</i>	<i>Average roughness, Ra</i>	<i>Average roughness, Rz</i>	<i>Units</i>
STAVAX ESR	Mirror polished	6.04	97.619	nm
SDL STA		5.201	113,818	nm
SDL 14		4.188	82.221	nm

Measured roughness of the different layers of grinded surfaces **Table 22**

<i>Layer</i>	<i>Surface condition</i>	<i>Average roughness, Ra</i>	<i>Average roughness, Rz</i>	<i>Units</i>
STAVAX ESR	grinded	0.279	2.454	μm
SDL STA		0.221	1,856	μm
SDL 14		0.186	1.112	μm

Measured roughness of the different layers of eroded surfaces **Table 23**

<i>Layer</i>	<i>Surface condition</i>	<i>Average roughness, Ra</i>	<i>Average roughness, Rz</i>	<i>Units</i>
STAVAX ESR	eroded	0.526	4.314	μm
SDL STA		1.226	6.738	μm
SDL 14		0.542	4.044	μm

The AFM images of the scanned surfaces for the three types of finishing are presented in the figures below. Fig. 5.23 – 5.25 show images of the mirror-polished surfaces of the base material (Fig. 5.23), a section welded with SDLSTA additive material (Fig. 5.24) and a section welded with SDL 14 (Fig. 5.25). It is evident that the surfaces have an identical shape. The deeper traces that can be seen in Fig. 5.23 and 5.24 are traces of the previous treatment in the polishing process. Their depth is about 25 nm, which is not visually noticeable and cannot be considered as a functional defect of the working surface.

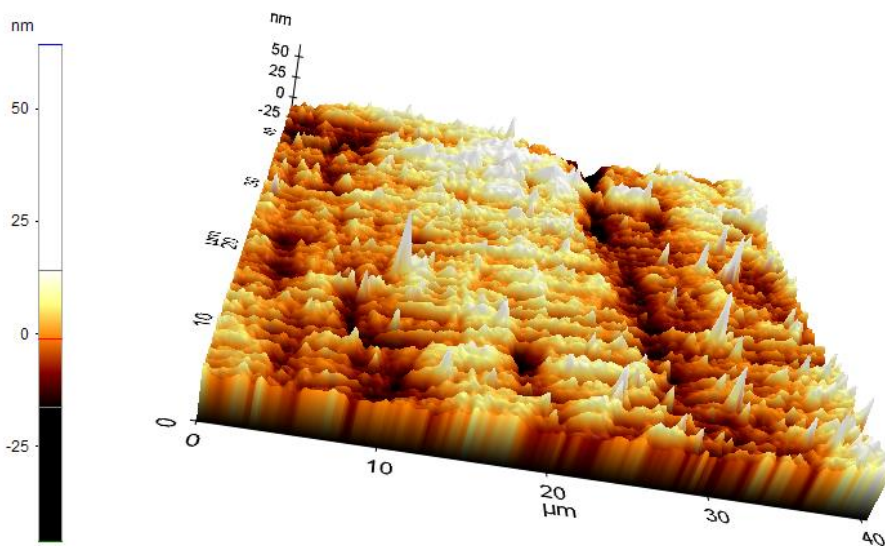


Fig.5.23. *Mirror-polished surface with STAVAX ESR base material.*

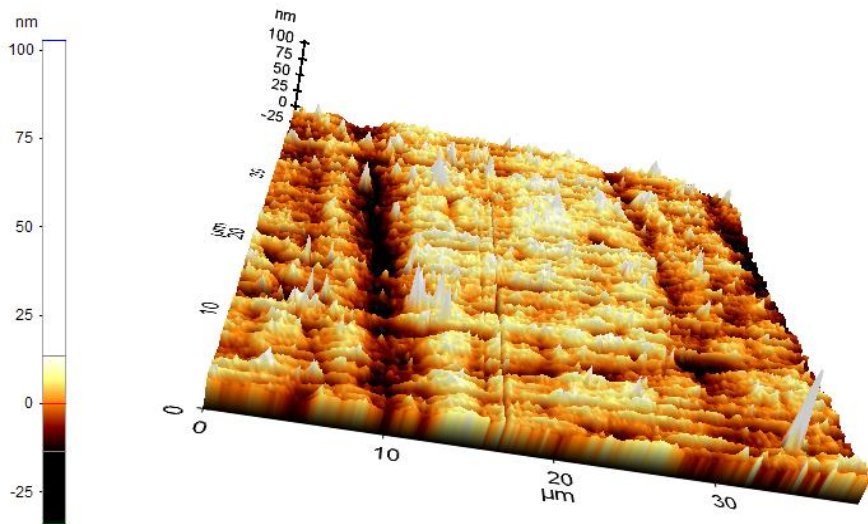


Fig.5.24. Mirror-polished surface, welded with SDLSTA additive material.

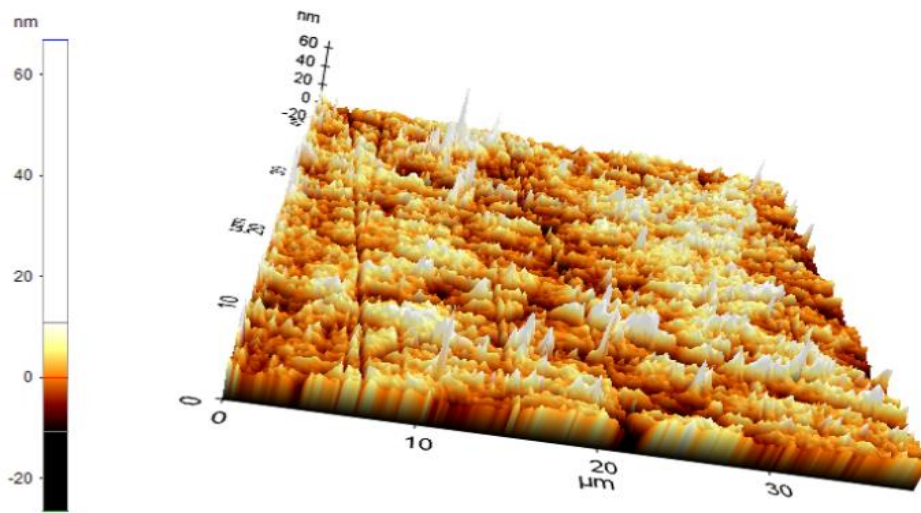


Fig.5.25. Mirror-polished surface, welded with additive material SDL 14.

Figures 5.26 – 5.28 present the scanned images of the grinded surfaces of the base material (Fig. 5.26), a section welded with SDLSTA additive material (Fig. 5.27) and a section welded with SDL 14 (Fig. 5.28). The difference between them is minimal.

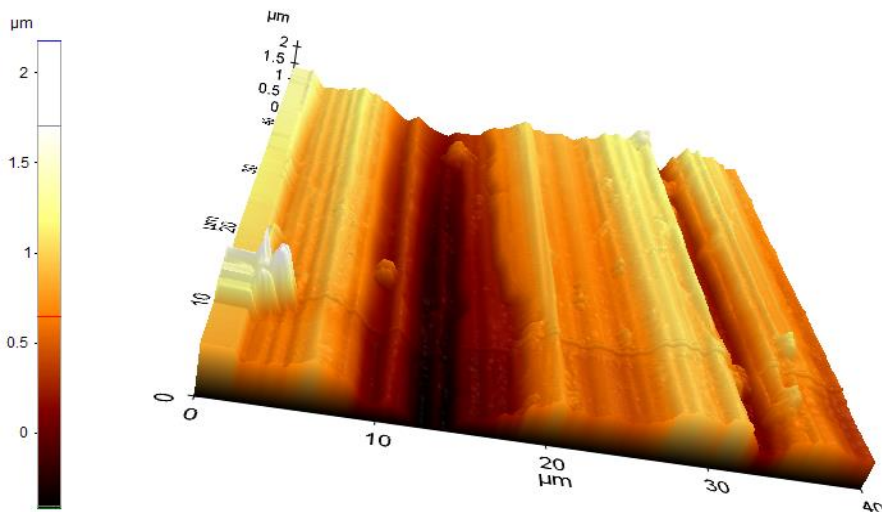


Fig.5.26. Grinded surface with STAVAX ESR base material.

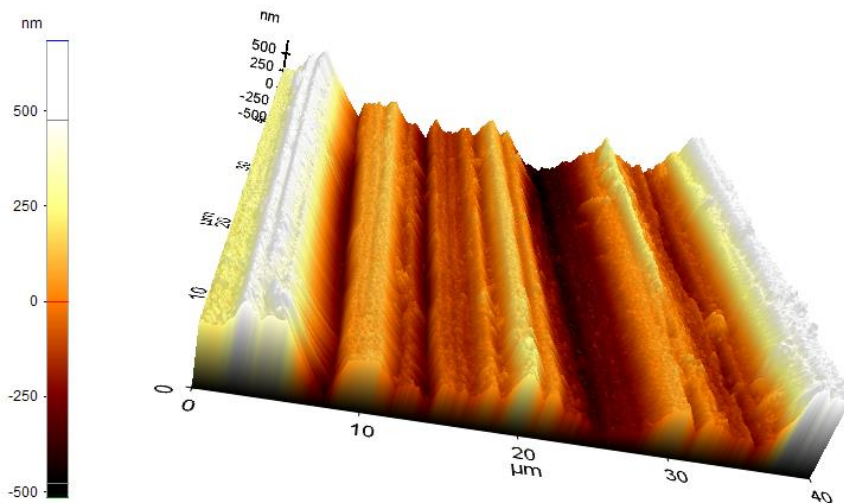


Fig.5.27. Grinded surface, welded with SDL STA additive material.

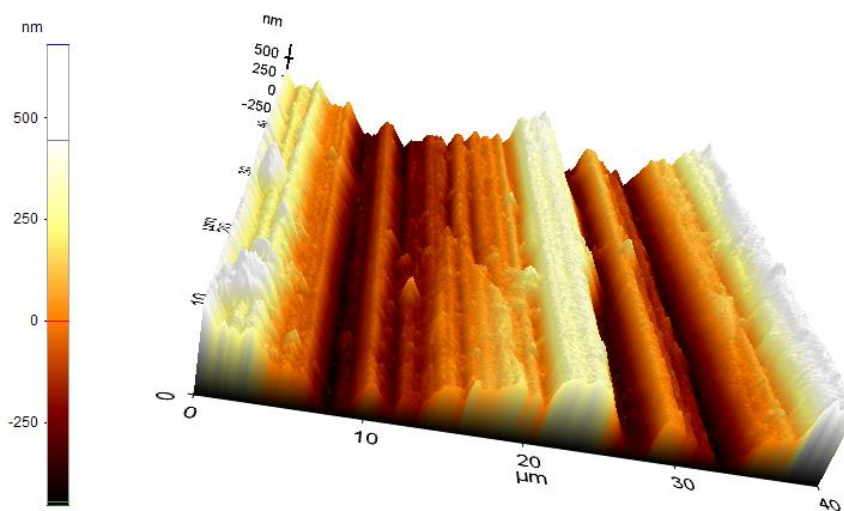


Fig.5.28. Grinded surface, welded with additive material SDL 14.

Figures 5.29 – 5.31 present images of eroded surfaces of the base material (Fig. 5.29), a section welded with SDLSTA filler material (Fig. 5.30) and a section welded with SDL 14 (Fig. 5.31), respectively.

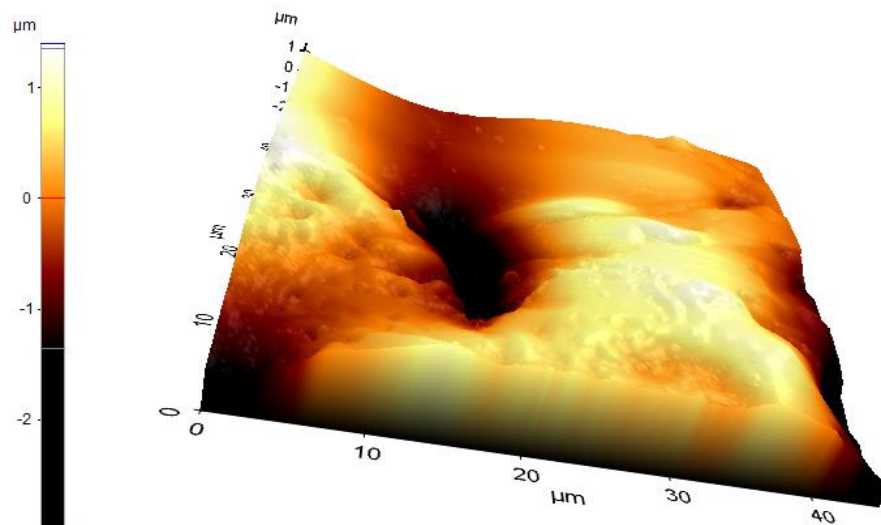


Fig.5.29. Eroded surface with STAVAX ESR base material.

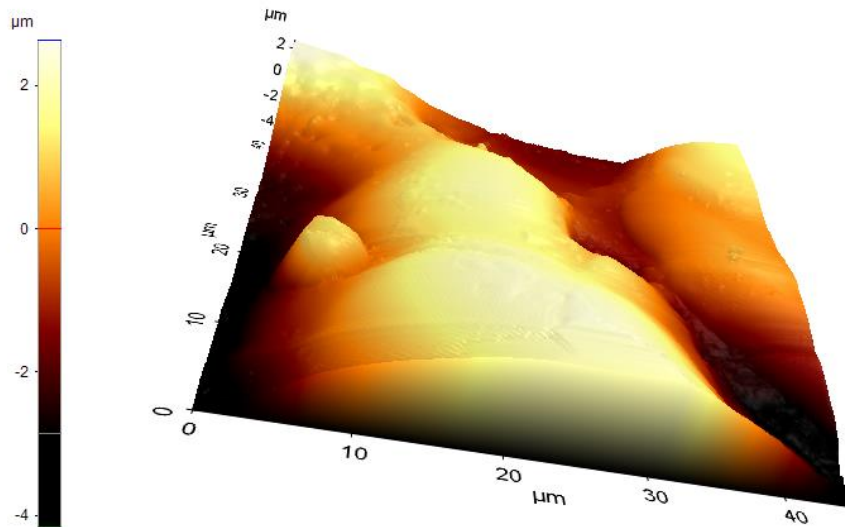


Fig.5.30. Eroded surface, welded with SDL STA additive material.

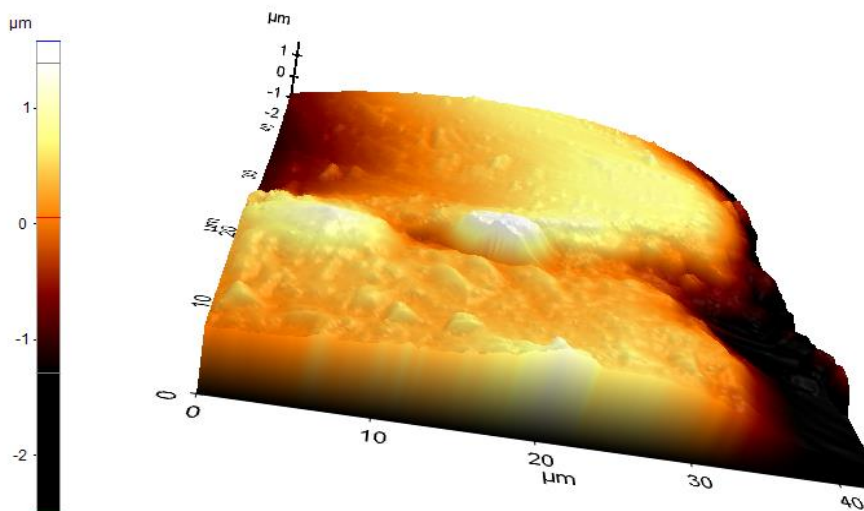


Fig.5.31. Eroded surface, welded with additive material SDL 14.

With this type of surface treatment, no visible differences are noticeable. Since this finishing treatment is the most widely used in the production of injection molds for plastic parts, it can be assumed that the laser welding method for the purpose of repairing active elements is very suitable.

5.4.3. Analysis of results

Welded surfaces lend themselves well to machining by grinding and electro-erosion. No appreciable difference in the roughness of the different layers was observed when processing the sections welded with SDL STA and SDL 14 additive material. The main problem is the appearance of weld creep, visible only in the mirror-polished areas. The measured roughness in the regions examined is identical for the different material types.

The measured hardness of the layer built with the additive material SDLSTA, which is specially designed for welding Stavax ESR steel, is close to the hardness of the base material. This shows that this method is suitable for repairing worn areas of injection molds, as the result of its application is the restoration of the working surfaces with a hardness close to the original.

The measured hardness of the layer built with SDL 14 is too low to build up areas worn due to the abrasive effect of the glass fibers in the polymers. However, this additive has a high toughness, which makes it suitable for crack repair.

Chapter 6. Practical methods for restoring the performance of defective injection molds

6.1. Laser crack filling

The laser welding method, in addition to repairing worn areas of active elements, can also be successfully used to repair cracks.

Copper or aluminum plugs are often used in practice to isolate the ends of the technological holes for the cooling circuits of the injection molds. As a result of the cyclic force and temperature loads, in combination with the different coefficients of thermal expansion of the steel and the plug material (Cu, Al), internal stresses appear, which develop into cracks - Fig. 6.1.



Fig.6.1. Leakage from the cooling circuits due to cracks in the area of the plugs

The following operations were performed to repair the cracks:

- Milling a channel in the crack area until it is completely removed;
- Filling the channel by laser welding with a additive material with increased toughness;
- Mechanical processing to remove excess weld metal and restore the hole surfaces in the plug area;
- Installation of a removable plug with an o-ring (Fig. 6.2), in order to eliminate the possibility of re-occurrence of stresses in the repaired area.



Fig.6.2. Removable plug with o-ring[124]

Conclusion: As a result of the measures taken, the problem was permanently eliminated until the injection mold resource was exhausted.

6.2. Restoration of work surfaces by sandblasting

The wear of the working surfaces of the injection molds due to the action of abrasive fillers in the melt leads to a deterioration in the appearance of the manufactured parts.

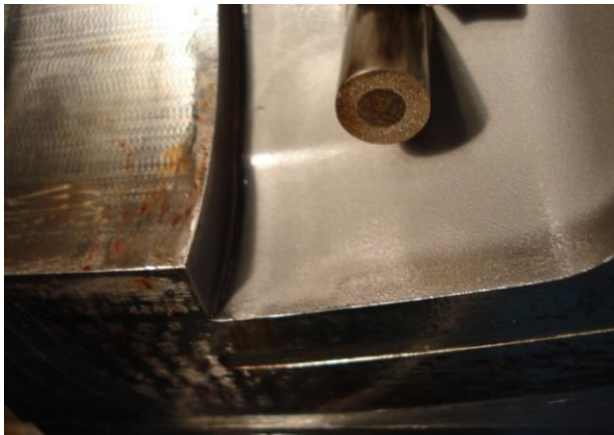


Fig.6.3. Abrasive wear on the working surface of an injection mold



Fig.6.4. Defective product

Figure 6.3 shows a worn section of an injection mold producing an angle grinder handle, as well as the product produced from it (Figure 6.4) with visible defects. The defects consist of worn edges of the mold and shiny spots, due to abrasive wear of the active part of the glass fibers in the granulate.

The material from which the active elements of the tool are made is low-carbon steel of the NAK 80 brand (manufactured by DAIDO Steel - Japan), with a measured hardness of 36 - 38 HRC and a chemical composition indicated in Table 24:

Chemical composition of steel NAK 80[129] *Table 24*

<i>C</i>	<i>Yes</i>	<i>Mn</i>	<i>Cr</i>	<i>Mo</i>	<i>Ni</i>	<i>Al</i>	<i>Cu</i>
0.12	0.3	1.5	0.3	0.3	3.2	1.0	1.0

The granulate intended for the production of parts with this injection mold is PA 6 with the trade name Durethan BKV 130. This granulate contains 30% glass fibers, which makes it highly abrasive to the steel of the injection mold. The estimated life cycle of the tool with the above materials does not exceed 250,000 - 300,000 cycles.

Actions have been taken to repair the injection mold as follows:

- Welding of worn areas with a pulsed TIG welding machine in order to restore the edges of the closing surfaces. For this purpose, an appropriate filler material was used;
- Cleaning the weld deposit affecting the working surface by milling with a CNC milling machine;
- Sandblasting of working surfaces with sand of appropriate grain size;
- Milling / grinding of the front closing surfaces;
- Production of a pilot series of parts after repair (Fig. 6.5).



Fig.6.5. Produced part after injection mold repair

As a result of repeating the measures taken three times over a period of about 300,000 cycles, the tool life was extended to 1,100,000 production cycles.

6.3. Extending the life of injection molds after cracks appear

Cyclic force and temperature loading of injection molds in certain cases leads to the appearance of cracks in vulnerable areas. Sometimes these cracks lead to the impossibility of continuing production and the need for major repairs of the tool.

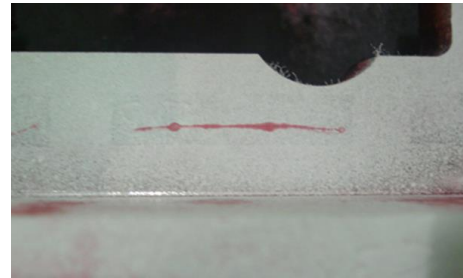
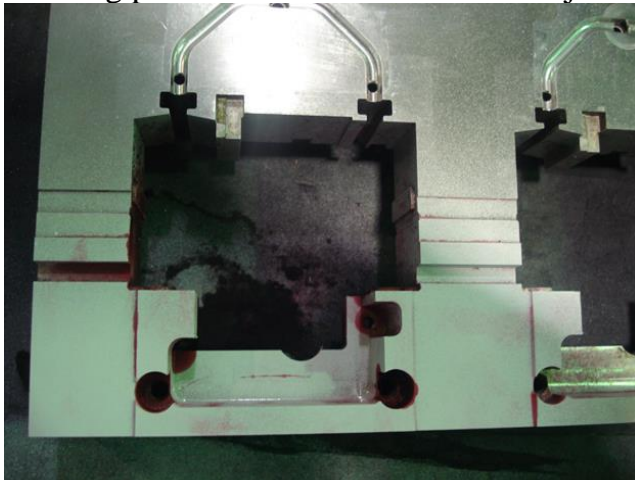


Fig.6.6. Crack in the mold (in red) localized after performing a non-destructive crack detection test BycoTest

Fig. 6.6 shows a mold with a water leak from the tempering channels to the active area of the tool. After inspecting the mold and using special preparations for non-destructive testing, it was found that the mold was cracked in the area colored red.

In order to continue the operation of the tool until a new mold was manufactured to replace the damaged one, the following measures were taken:

- Mechanical cleaning of the cooling channels in the crack area from rust and lime scale deposits;
- Manufacturing of a special thin-walled tube with a nominal outer diameter equal to the nominal bore diameter;
- Installation of seals at both ends of the pipe in channels;
- Applying thermally conductive paste to the outer diameter of the pipe;
- Installation of the pipe in the mold cooling hole;
- Assembling the tool and starting production.

CONCLUSION

This dissertation is dedicated to the study and development of methods for increasing the service life of plastic molding tools. A detailed analysis of the factors leading to wear of

injection molds, as well as the influence of structural, mechanical, thermal and chemical loads on their service life, has been carried out. A set of methodologies for assessing wear resistance has been presented, process simulations and design optimization analyses have been carried out.

As a result of the theoretical, simulation and experimental studies, specific solutions have been formulated to extend the tool life. The effectiveness of multilayer hard coatings and laser surfacing for increasing wear resistance has been proven, as well as the role of surface topography for the durability of working surfaces. At the same time, practical methods for restoring defective tools have been proposed, which have high applicability in industrial practice.

The work brings together national and international experience and outlines clear guidelines for improving the quality and extending the life of injection molding tools.

CONTRIBUTIONS OF THE DISSERTATION

Scientific and applied contributions

1. It has been shown that the specific wear rate of the Ti/TiN/TiCN multilayer hard coating applied to Stavax ESR steel decreases with increasing load.
2. It has been found that preliminary mechanical and thermal treatment before applying a Ti/TiN/TiCN coating to Stavax ESR steel has a significant impact on the wear resistance, with hardened steel with polished surfaces having the lowest wear intensity.
3. It has been proven that the topography of laser-welded surfaces in the three types of finishing treatments (grinding, electrical discharge machining and mirror-polishing) does not differ from that of the base material.

Applied contributions:

1. It has been proven that by simulating the injection molding process, it is possible to determine the areas of the molding surfaces that are subject to intense wear, as well as the areas in which a local excess of the temperature of the liquid polymer above the upper limit of its operating range may occur.
2. Practical methods for laser welding cracks in critical areas, including cooling channels, are proposed, which can restore the operability of damaged injection molds.
3. It has been proven that the hardness of laser-welded layers with SDLSTA alloy is comparable to that of the base material, making them suitable for the restoration of worn areas.
4. A technology for restoring worn areas by welding and sandblasting, applicable in real production conditions, has been proposed.

List of publications included in the dissertation

- A1. **Simov M. D.**, Rupetsov V. S., Pashinski Ch. O., Mechanical tests of gradient Ti/TiN/TiCN hard coating intended for tool production, *Alternative Energy Sources, Materials & Technologies (AESMT'22)*, Volume 4, 2022, ISSN 2603-364X
- A2. **Simov M.**, Rupetsov V., Iacobescu G., Comparative analysis of properties of laser welded steel layers on substrate – Stavax ESR steel, *Journal of the Balkan Tribological Association*, Vol. 31, No 3, 463–473, 2025, ISSN 1310-4772
- A3. **Simov M.**, Warpape compensation in plastic parts by pre-adjusting the shapes using Moldex 3D simulation software, *Journal of the Balkan Tribological Association*, Vol. 31, Issue 1, pp. 15–23, 2025, ISSN 1310-4772